Catalysis Today xxx (xxxx) xxx–xxx

Contents lists available at ScienceDirect

Catalysis Today

journal homepage: www.elsevier.com/locate/cattod

Aqueous phase hydrogenation of furfural using carbon-supported Ru and RuSn catalysts

Juan J. Musci[a], Andrea B. Merlo[a], Mónica L. Casella[a,b,*]

[a] CIT UNNOBA, CONICET, Universidad Nacional del Noroeste de la Provincia de Buenos Aires Newbery 261, 6000 Junín, Provincia de Buenos Aires, Argentina
[b] CINDECA (CCT La Plata-CONICET, UNLP), Universidad Nacional de La Plata, Facultad de Ciencias Exactas, 47 N◦257, 1900 La Plata, Argentina

ARTICLE INFO

Dedicated to the memory of Professor Osmar Ferretti on occasion of the tenth anniversary of his early death.

Keywords:
Aqueous phase hydrogenation
Biomass
Furfural
Surface organometallic chemistry
RuSn

ABSTRACT

The aqueous phase hydrogenation (APH) of furfural was studied over carbon-supported monometallic Ru and bimetallic RuSn catalysts at 90 °C and 1.25 MPa. Tin was added via Surface Organometallic Chemistry on Metals techniques and its effect was a function of the Sn/Ru atomic ratio. Thus, the addition of Sn in a Sn/Ru ratio of 0.4 promoted the $C{=}O$ hydrogenation reaching a selectivity towards furfuryl alcohol over 85% throughout the course of the reaction. A higher concentration of tin does not improve the situation. It seems to be a compromise between the dilution of Ru sites, active for the hydrogenation reaction, and the promoting effect of Sn. TEM, TPR and XPS characterization indicate the strong interaction between Ru and Sn in all the bimetallic catalysts. Finally, the reuse of the catalyst was analyzed.

1. Introduction

The transformation of biomass into fuels and chemicals has become an increasingly popular alternative as a way to mitigate global warming and diversify energy sources [1]. Biomass is a renewable resource, generally considered neutral from the point of view of the carbon cycle, and fuels derived from it are generally burned cleaner than fossil fuels. It is estimated that biomass could provide about 25% of the world's energy needs [2]. In addition, biomass is also a source of valuable chemicals, pharmaceuticals and food additives [3]. There are several types of biomass that can be converted into fuels and chemicals. Examples include wood and wood wastes, agricultural crops, agricultural waste, waste from food processing operations, etc. [4].

The conversion of biomass into energy and chemicals involves the use and development of various types of processes (physical, chemical and enzymatic). Thus, biomass can be burned, transforming it into biogas and by means of a biochemical process bioalcohol can be obtained. Finally, through diverse chemical processes not only fuels (for example, biodiesel) can be obtained, but also an important number of chemical products can be synthesized.

The reorganization of an economy based on biological raw materials requires new approaches in research and development, production and economy. Biorefineries combine the technologies needed to generate intermediate and final industrial products from biological raw materials. Nowadays, the most favored biorefineries regarding research and development are the so-called “biorefinery of agricultural products” (cereals, corn), “green biorefinery” (wet biomass, such as green grass, alfalfa, clover or immature cereal) and “lignocellulosic biorefinery” (dry biomass and wastes containing cellulose) [4].

Among potential large-scale industrial biorefineries, lignocellulosic biorefinery will most likely be the most rapidly developed. This is because, on the one hand, the raw material to be used is easily available and abundant (straw, cane, grass, wood, wastepaper, etc.) and, on the other hand, the products of its conversion have a good position within the traditional petrochemical industry and, therefore, it is expected to be the same in future bioproduct markets [4].

Lignocellulose is the main component of the cellular wall of plants. It consists of three primary fractions of more or less defined composition: (a) hemicellulose (25–35%) which is a complex polymer of heteropolysaccharides composed of pentoses and hexoses forming branched chains; (b) cellulose (40–50%), a polymer formed by glucose units linked by β-glucosidic bonds and (c) lignin (15–20%), a phenol polymer [5,6]. By acid-catalyzed hydrolysis of hemicellulose, it is possible to obtain furfural, among other molecules of interesting properties.

Furfural is a substance with great potential as a renewable chemical platform for the production of bioproducts and biofuels [7]. Although at present 65% of the production of furfural is intended for the synthesis of furfuryl alcohol, it is a very versatile compound from which a wide variety of chemicals can be obtained. Among these are furan and furoic

---

* Corresponding author at: CINDECA (CCT La Plata-CONICET, UNLP), Universidad Nacional de La Plata, Facultad de Ciencias Exactas, 47 N°257, 1900 La Plata, Argentina.
E-mail address: casella@quimica.unlp.edu.ar (M.L. Casella).

http://dx.doi.org/10.1016/j.cattod.2017.04.063
Received 12 December 2016; Received in revised form 23 March 2017; Accepted 30 April 2017

Please cite this article as: Musci, J.J., Catalysis Today (2017), http://dx.doi.org/10.1016/j.cattod.2017.04.063

Table 1
Reaction conditions employed in the preparation of the bimetallic catalysts through SOMC/M techniques. Initial and final $SnBu_4$ concentration measured by gas chromatography and atomic ratio between Sn and Ru.

Catalyst	T(°C)[a]	Wt. (g)[b]	Reaction time (h)	C_i (mmol L^{-1})[c]	C_f (mmol L^{-1})[c]	Sn/Ru[d]
RuSn0.1/C	90	1.5	5.5	4.2	1.1	0.14
RuSn0.2/C	120	1.2	7	6.1	2.9	0.16
RuSn0.4/C	120	3.0	5.5	60.8	54,1	0.45
RuSn0.8/C	150	2.0	5.5	19	7,1	0.80

[a] Reaction temperature.
[b] Mass of monometallic catalysts employed.
[c] $SnBu_4$ concentration normalized to 1 g of Ru/C (C_i = initial concentration and C_f = final concentration).
[d] Atomic ratio.

acid. These products are used to increase the octane number of gasolines and as raw material and intermediate products for the synthesis of medicines and perfumes, respectively. There are also catalytic routes that, starting from furfural, allow the synthesis of polyamides, rubber and different types of Nylon, many of them with industrial application and which are currently derived from the petrochemical industry [8].

In particular, this work is focused on obtaining furfuryl alcohol, which is used primarily as an ingredient in the manufacture of various chemical products, such as foundry resins, adhesives, and wetting agents, among other uses [9]. Conventional preparation of furfuryl alcohol is carried out by catalytic hydrogenation of furfural, either in liquid or in vapor phase. [10,11]. The liquid phase reaction occurs with moderate activity towards furfuryl alcohol on a copper chromite catalyst, this being the most commonly used method of production. The reaction proceeds at high pressures and elevated temperatures, and has the great disadvantage of the toxicity of the copper chromite catalyst. To overcome this drawback, a wide variety of catalysts have been investigated for this reaction [12,13].

In order to obtain furfuryl alcohol, the aqueous phase catalytic hydrogenation (APH) of furfural was employed. This is a fundamental step in the aqueous phase processing of biomass, which allows its conversion into fuels and chemicals. Through APH, several functional groups can be hydrogenated, for instance C═O bonds, C═C bonds, hydroxyl or furan rings, etc. [14].

Hydrogenation reactions are usually carried out on catalysts based on Group VIII metals (Ru, Rh, Pd, Os, Ir, Pt) because of their ability to reduce the carbonyl group. However, the activity and selectivity of these catalysts very often need to be enhanced by adding an appropriate promoter [15,16]. Among noble metals, ruthenium appears as a promising active phase when modified by a second metal, especially tin. For example, it has been shown that the addition of tin onto a Ru/SiO_2 catalyst increases its selectivity to the hydrogenation of the C═O bond of crotonaldehyde, forming crotyl alcohol [17]. Also, unsaturated fatty acids and their esters have been successfully hydrogenated to their unsaturated alcohols over supported Ru-Sn catalysts [18,19].

This paper aims to study the catalytic aqueous phase hydrogenation of furfural, employing Ru-based heterogeneous catalysts supported on activated carbon. In order to improve the performance of this system, the effect of the addition of Sn as a promoter of conversion and selectivity was analyzed. The addition of tin to obtain RuSn bimetallic catalysts was carried out using techniques derived from the Surface Organometallic Chemistry on Metals (SOMC/M). These techniques allow the obtention, under mild reaction conditions, of highly dispersed bimetallic catalysts with well-defined particle sizes and surface composition.

2. Experimental

2.1. Catalyst preparation

A Ru catalyst, with a ruthenium loading of 3 wt.%, was prepared by impregnation with excess solution on a commercial activated carbon (C) (NORIT, ground and sieved to 60–100 mesh). The preparation procedure consisted of weighing the calculated amount of the ruthenium salt, $RuCl_3.xH_2O$ (*Aldrich*), which was dissolved in acetone in a liquid/solid ratio of 5:1. The system was left in contact for 24 h and then was dried in an oven at 60 °C for 1 h. Finally, it was washed until complete elimination of chloride ions (determined with $AgNO_3$). Before use, the catalyst was activated by in H_2 flow for 2 h at 300 °C, which is the temperature required to obtain the full reduction of ruthenium [20]. This catalyst was designated Ru/C.

RuSn bimetallic catalysts with Sn/Ru molar ratio between 0.1 and 0.8 were prepared by controlled surface reactions, using a methodology derived from SOMC/M techniques. According to this procedure, the previously reduced Ru/C catalyst was reacted with a solution of Sn $(C_4H_9)_4$ ($SnBu_4$, *Sigma-Aldrich*) in a paraffinic solvent. The reaction was carried out in a H_2 atmosphere at 90, 120 or 150 °C using or *n*-decane as solvent, depending on the reaction temperature. Once the reaction had finished, the liquid phase was separated and the solid was repeatedly washed with *n*-heptane under a N_2 flow. Then, the catalysts were reduced in a H_2 flow at 500 °C for 2 h. This temperature assures obtaining bimetallic phases by elimination of all the butyl groups of the $SnBu_4$ employed as tin precursor [21]. The so-obtained bimetallic systems were designated RuSny/C, where *y* values (0.1, 0.2, 0.4 and 0.8) represents the nominal Sn/Ru molar ratio. Table 1 lists all the bimetallic catalysts prepared, the reaction conditions employed in each case, including the initial and the final $SnBu_4$ concentration measured. It also indicates the atomic ratio between the two metals, which varied between 0.14 and 0.80.

2.2. Support and catalyst characterization

Surface area analysis was used to establish specific surface area (S_{BET}) and pore volume (V_P) of the support by N_2 physisorption at −196 °C using a *Micromeritics Accusorb 2100E* equipment. Surface area was calculated by the BET equation and the pore volume was estimated using the adsorption branch of the isotherm curve at $P/P_0 = 0.98$ single point.

Ru content was determined by Atomic Absorption Spectroscopy (AAS). Prior to the analysis, the sample was digested and $LaCl_3$ (*Sigma-Aldrich*) was added to eliminate interferences from HCl. A *Perkin Elmer AAnalyst 100* atomic absorption spectrometer was used to analyze the samples, using an acetylene/air flame and a hollow cathode lamp.

The tin content in the $RuSn_y/C$ bimetallic catalysts was determined by GC analysis, measuring the difference between the initial and the final concentration of $SnBu_4$ in the impregnating solution. A *Varian CP-800* gas chromatograph, equipped with a FID detector and a Factor Four (VF-1 ms, 15 m × 0.25 mm ID DF = 0.25) capillary column was employed.

Temperature-Programmed Reduction (TPR) experiments were performed in a laboratory-constructed equipment. A 50 mg sample was placed in a 6 mm diameter quartz reactor and purged with Ar for 20 min at 20 °C to remove impurities and water contained in the catalyst. Then, the sample was heated from room temperature to 700 °C at a heating rate of 10 °C/min with a reductive mixture composed of 5 vol.% H_2 in Ar. A *Shimadzu GC-8A* gas chromatograph equipped with a thermal conductivity detector (TCD) was used for measuring hydrogen consumption. The samples were dried at 105 °C and then calcined at 500 °C for 2 h before being subjected to TPR analysis.

Transmission electron microscopy (TEM) micrographs were obtained with a *JEOL 100 CX II* microscope. The samples were prepared by ultrasonic dispersion of the previously crushed powders in distilled water. Then, a droplet of the dispersion was placed onto a carbon-coated copper grid. Frequency histograms of Ru particle sizes have been estimated by measuring the diameter of at least 100 particles on each sample. The mean particle size (d_{TEM}) was obtained from the following expression (mean volume-area diameter):

$$d_{TEM} = \frac{\sum_i n_i d_i^3}{\sum_i n_i d_i^2}$$

where n_i is the number of particles with size d_i.

X-ray photoelectron spectroscopy (XPS) analysis were performed on a *Specs Multi-technique system (SPECS)* equipped with a dual Mg/Al X-ray source and a PHOIBOS 150 hemispherical analyzer operating in the Fixed Analyzer Transmission (FAT) mode. The spectra were obtained with a pass energy of 30 eV and a Mg anode operated at 85 W. The working pressure in the analyzing chamber was less than 5.9×10^{-7} Pa. Samples were supported on double-sided tape Cu and evacuated to ultra-high vacuum for at least two hours before reading. The data treatment was performed with the *Casa XPS* program (Casa Software Ltd., UK). The peak areas were determined by integration employing a Shirley-type background and the peaks were considered as a Gaussian/Lorentzian mix of variable proportion.

2.3. Catalytic tests

Several tests with different catalyst masses and stirring rates were carried out in order to assure that the hydrogenation tests were measured under a kinetic regime.

The aqueous phase hydrogenation of furfural was performed in a high pressure reactor (*Berghof BR-100*) at a hydrogen pressure of 1.25 MPa and a temperature of 90 °C. Typically, 250 mg catalyst (60–100 mesh) was placed into the reactor, together with 0.45 mL of furfural and 50 mL of water. The evolution of the reaction was followed through the analysis of the liquid products by gas chromatography. A *Varian CP-3800* gas chromatograph equipped with a FID detector was used. The capillary column employed was a CP Wax 52 CB (30 m; 0.3 mm d.i.). The reaction products were identified by GC–MS (*GCMS QP-2010 ULTRA*, Shimadzu, Japan).

The conversion of furfural and the selectivity of the products were calculated using the following expressions:

$$x(\%)_{FF} = \frac{C_{FF}^0 - C_{FF}^t}{C_{FF}^0} 100$$

where x_{FF} is the furfural conversion, C°_{FF} is the initial molar concentration of furfural and C_{FF}^t its molar concentration at time t (min). The selectivity to compound i (S_i) was determined as indicated in the following equation:

$$S(\%)_i = \frac{C_i^t}{\sum_{i=1}^n C_i^t} 100$$

where C_i^t is the molar concentration of compound i at time t (min).

The initial rates of furfural conversion (r_i, $\mathrm{mmol_{FF}\ gRu^{-1}\ min^{-1}}$) were estimated from the slope of the straight lines obtained from x_{FF} vs. time (Fig. 5) considering data at $x_{FF} < 10\%$. In the case of $RuSn_{0.8}/C$ catalyst, r_i was calculated after correction of the induction period.

2.4. Catalyst reusability

The behavior of the Ru/C, $RuSn_{0.4}/C$ and $RuSn_{0.8}/C$ catalysts in successive hydrogenation reactions was analyzed. For this purpose, a series of experiments were carried out in which, after 420 min of reaction (under the experimental conditions explained in the previous section), the catalyst was washed with distilled water and reused until three cycles of hydrogenation were completed.

3. Results and discussion

3.1. Preparation of RuSny/C catalysts

The RuSny/C catalysts employed in this paper were obtained by a surface-controlled reaction between the reduced Ru/C monometallic catalyst and a solution of $SnBu_4$ in a paraffinic solvent (*n*-heptane or *n*-decane). This technique, which consists of the reaction between a supported transition metal with an organometallic compound of metals such as Sn, Ge or Pb in a H_2 atmosphere, allows the control of the different steps of the catalyst preparation, giving rise to reproducible solids both from the point of view of their structure and catalytic performance [22–24]. The preparation reaction can be explained by a two-step process: in the first one, the organic groups are anchored to the metallic surface giving rise to an organometallic system (temperature between 90 and 150 °C) and in the second one, the formation of a bimetallic phase takes place after all the organic fragments have been released (temperature between 150 and 500 °C). The reactions taking place in these two stages can be represented by the following equations:

$$Ru/C + ySnBu_4 + \frac{xy}{2}H_2 \rightarrow Ru(SnBu_{4-x})_y/C + xyBuH$$

$$Ru(SnBu_{4-x})_y/C + \frac{(4-x)y}{2}H_2 \rightarrow RuSn_y/C + (4-x)yBuH$$

The specificity of the reactions that take place during the preparation of bimetallic catalysts using SOMC/M techniques has been proven by several authors, concluding that all the tin added is selectively deposited on the supported metal [21,25]. Thus, if the surface of the base monometallic catalyst (in our case Ru/C) is covered with H_2, the reaction of tetra-*n*-butyl tin leads to its selective deposit on the metal particle and the support is untouched. No reaction occurs on the support in such conditions. In this paper, this fact was confirmed by performing a blank reaction: a given amount of the carbon support was contacted with $SnBu_4$ solutions at the different reaction temperatures tested (90, 120 and 150 °C). For all the cases, it was found that the amount of $SnBu_4$ fixed was less than 1 wt.%, after 5 h of reaction. The reaction between $SnBu_4$ and the reduced Ru/C catalyst was followed by gas chromatography, measuring the variation of the concentration of $SnBu_4$ in the impregnating solution as a function of time. Fig. 1 shows the variation of the Sn/Ru molar ratio as a function of time for the four prepared bimetallic catalysts. The reaction temperature and the contact time between the monometallic catalyst and the organotin compound are two fundamental variables in obtaining a catalytic system with a determined Sn/Ru ratio, as has been previously demonstrated by our research group when applying this technique to different supported transition metals [26]. It has also been determined that the initial concentration of the $SnBu_4$ solution has no effect on the maximum amount of Sn fixed. Thus, the saturation value depends only on the temperature, increasing when it increases [21,27].

3.2. Characterization of support and catalysts

The surface study of the carbon support by N_2 physisorption indicated that this support had a S_{BET} of $1000\ m^2\ g^{-1}$ and a pore volume of $0.53\ m^3\ g^{-1}$. TEM analysis confirmed the presence of uniform-sized particles with a mean volume-area diameter of 1.1 nm

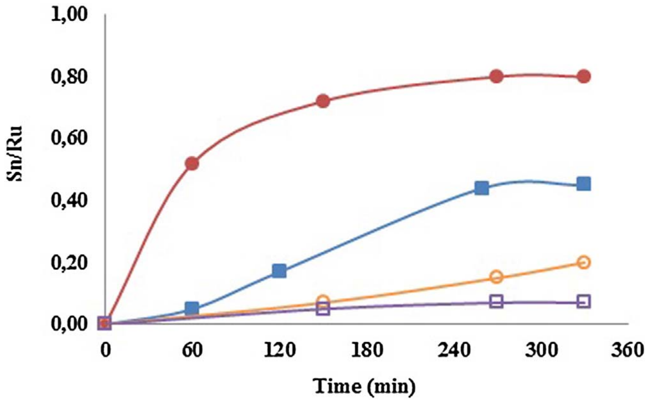

Fig. 1. Amount of tin fixed (measured as Sn/Ru ratio) as a function of time (min): (●) Sn/Ru = 0.8 (*n*-decane, 150 °C), (■) Sn/Ru = 0.4 (*n*-heptane, 120 °C), (○) Sn/Ru = 0.2 (*n*-heptane, 120 °C) and (□) Sn/Ru = 0.1 (*n*-heptane, 90 °C).

(Fig. 2(a)). The Ru dispersion for the monometallic catalyst was 81%, calculated by the following equation [28]:

$$D_{Ru} = \frac{0.91}{d_{TEM}}$$

where D_{Ru} is the dispersion of the ruthenium particles and d_{TEM} is the mean volume-area diameter obtained from TEM measurements. After the addition of Sn, the average particle size increased to 2.7 nm and 2.2 nm for $RuSn_{0.4}/C$ and $RuSn_{0.8}/C$ catalysts, respectively (Fig. 2(b) and (c)). This increase in particle size can be assigned in part to the selective deposit of tin on ruthenium, according to what is well established in the literature for other catalytic systems analogous to those studied here [22,26]. However, the contribution of the sintering of the ruthenium particles cannot be neglected. The thermal treatment to which the $Ru(SnBu_{4-x})_y/C$ system is submitted in order to remove the organic moieties and obtain the bimetallic catalyst would be responsible for that sintering.

TPR was used to determine the reducibility of the prepared catalysts. The TPR profile of all the studied catalysts as well as that of the carbon support are displayed in Fig. 3. Ru/C catalyst presents a wide region of H_2 consumption between 80 and 260 °C, where it is possible to identify three maxima: i) the peak centered around 140 °C may be assigned to the decomposition of the oxygen-containing functional groups of the support surface, ii) the second peak, which appears around 190 °C, corresponds to the reduction of Ru(III) to Ru(0) and iii) the peak at 250 °C and the wide H_2 consumption band at higher temperatures can be assigned to the gasification of surface carbon atoms located around the metal particles [29]. Concerning the TPR profiles of the bimetallic catalysts, as can be observed, there is an important shift of the H_2 consumption peak assigned to the reduction of Ru(III) to Ru(0) to lower temperatures. This signal appears at 90 and 100 °C for $RuSn_{0.4}$ (curve (b)) and $RuSn_{0.8}$ (curve (c)), respectively. In the temperature range between 300 and 400 °C appears a wide peak of H_2 consumption, that could be assigned to the reduction of Sn(II,IV). Taking into account that the reduction of bulk tin oxides occurs at temperatures above 630 °C, this shift of the signal would be indicating a strong interaction between ruthenium and tin. Finally, the H_2 consumption starting from 500 °C can be associated to the formation of methane through the carbon reduction of the support [30].

X-ray photoelectron spectroscopy (XPS) was employed to investigate the oxidation state of Ru and Sn and the surface composition of the catalysts. The binding energies (BE) of the Ru3d, C1s, Sn3d and O1s levels for Ru/C, $RuSn_{0.4}$ and $RuSn_{0.8}$ catalysts are reported in Table 2. The values of BE of Ru $3d_{5/2}$ registered for the reduced catalysts were attributed to the presence of Ru mostly in the metallic form, although the downwards shift in its BE in the bimetallic catalysts compared to Ru/C (280.5 eV) is indicative of the existence of an electronic effect of tin over ruthenium. This results go in the same direction as those reported for tin-promoted platinum catalysts prepared by SOMC/M techniques [31]. Concerning tin oxidation state, the Sn $3d_{5/2}$ peak obtained by XPS contains two contributions (Fig. 4). The first with a binding energy of around 485 eV is assigned to Sn(0) [32]; the second contribution corresponds to Sn(II,IV), with a binding energy centered around 487 eV [33]. The fraction of metallic tin is 20.8% and 29.9% for $RuSn_{0.4}$ and $RuSn_{0.8}$, respectively. The existence of bimetallic RuSn phases (even alloys) could be inferred from the presence of metallic tin

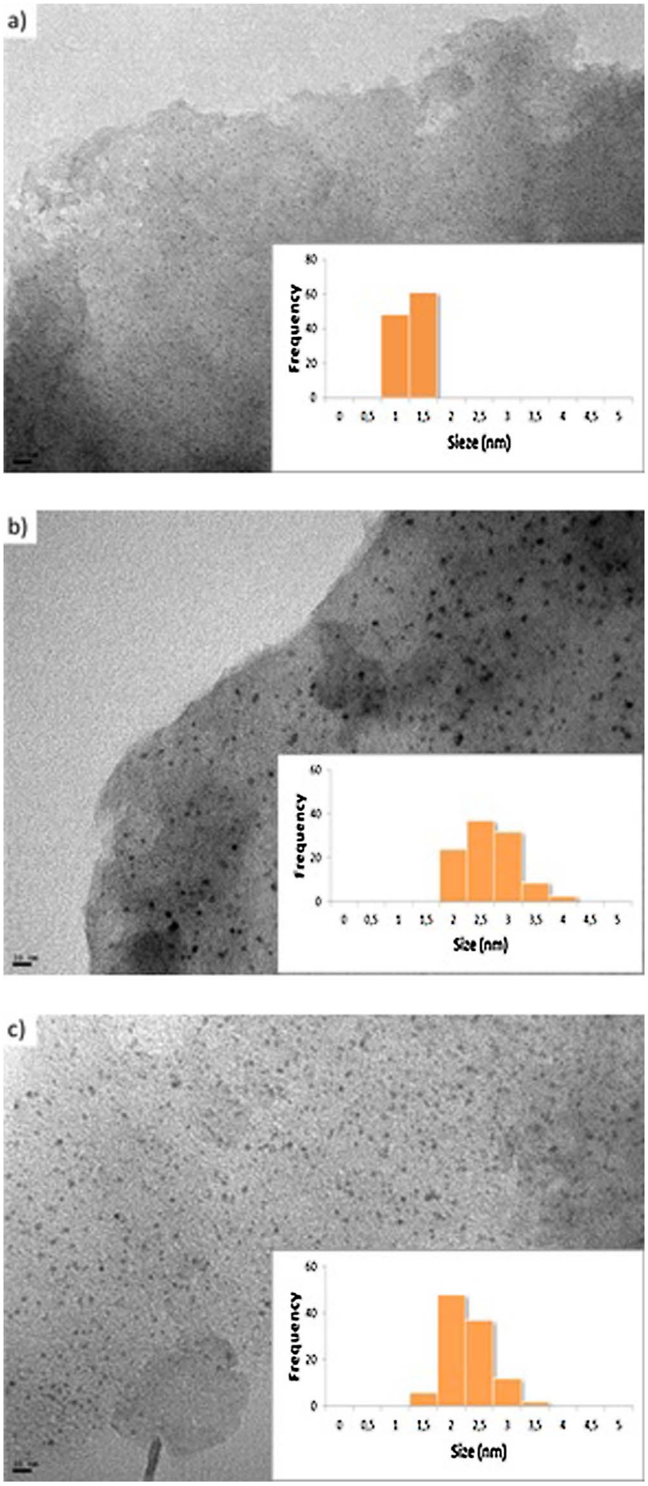

Fig. 2. TEM micrographs (magnification: 450000X) and particle size distribution of the Ru species (inserts). (a) 3 wt% Ru/C; (b) $RuSn_{0.4}/C$ and (c) $RuSn_{0.8}/C$.

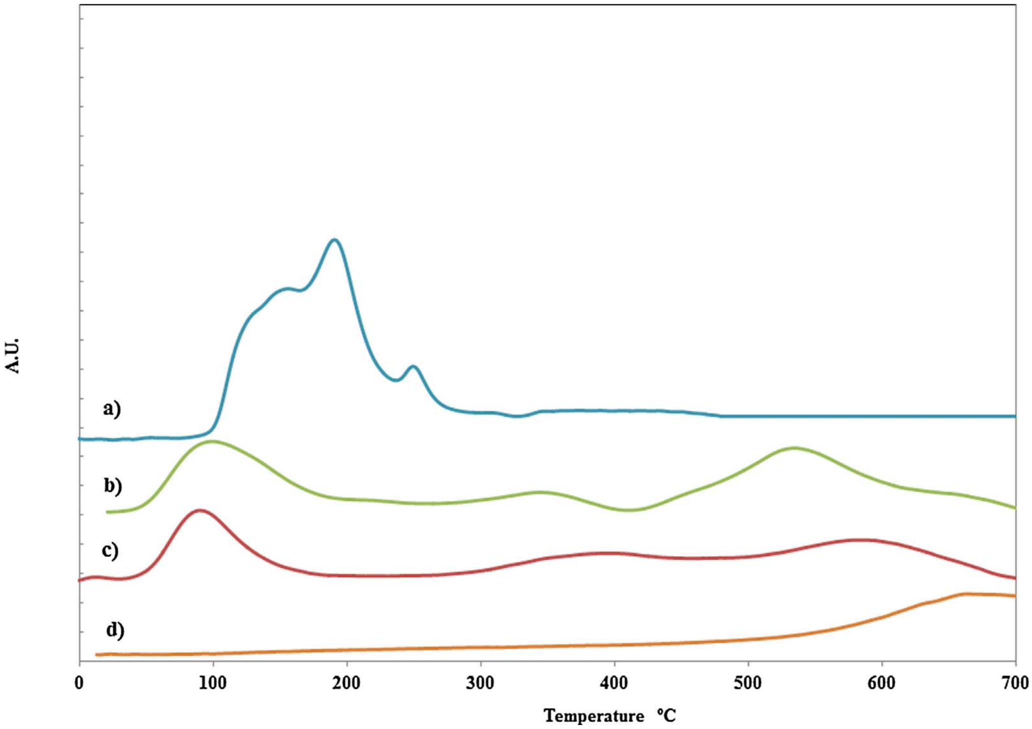

Fig. 3. Temperature-programmed reduction (TPR) profile for (a) Ru/C, (b) RuSn0.8/C and (c) RuSn0.4/C catalysts; and (d) carbon support.

Table 2
Binding energies (BE) of core levels of Ru/C, RuSn0.4/C and RuSn0.8 catalysts measured by XPS.

Catalyst	BE (eV)			
	$Ru3d_{5/2}$	C1s	$Sn3d_{5/2}$	O1s
Ru/C	280.5	284.8	–	532.2
$RuSn_{0.4}/C$	279.4	284.8	485.5 (20.8%) 486.9 (79.2%)	532.3
$RuSn_{0.8}/C$	279.6	284.7	485.4 (29.9%) 486.8 (70.1%)	532.4

in bimetallic catalysts [31].

3.3. Aqueous phase hydrogenation of furfural (FF)

The aqueous phase hydrogenation of FF was carried out with Ru/C, $RuSn_{0.4}/C$ and $RuSn_{0.8}/C$ catalysts. In Fig. 5, the conversion of FF as a function of time for such catalysts is observed. FF conversion after 400 min reaction reached values between 85 and 95%, indicating that the three tested catalysts were active in this reaction. These are promising results, especially taking into account that the reaction conditions used in this work are milder than those normally found in the literature [34,35].

The initial reaction rates (r_i) and the turnover frequencies (TOF) for the three studied catalyst systems are presented in Table 3. The r_i values obtained in this case are much lower than those obtained in the FF hydrogenation with platinum-based catalysts and using 2-propanol as solvent, for example [27]. The characteristics of water as a solvent, in this case its polarity, can strongly influence the catalytic activity during FF hydrogenation. For instance, water affects the solubility of hydrogen in the reaction media and competes with FF for the adsorption on the catalyst. This last fact could be responsible for the less efficient adsorption of furfural on the catalyst and consequently, of its lower hydrogenation rate. It could also be the cause of the existence of an induction period in the evolution of FF conversion, which is particularly appreciable in the catalyst with the highest Sn content. The effects of water on the catalytic hydrogenation of FF has been systematically studied by several authors, although no homogeneous results have been reached [36,37].

Differences in the exposed metallic Ru sites in the three studied catalysts were taken into account through TOF values. The addition of tin in a Sn/Ru atomic ratio of 0.4 led to an increase in the catalytic activity. This result could be assigned to the fact that tin reduces the hydrogen adsorption intensity on the ruthenium surface, increasing the availability of hydrogenation sites. This explanation has been proposed, among others, by Zhang et al., who proposed that the reactivity of platinum catalysts in furfural hydrogenation could be improved by decreasing H_2 adsorption strength through the addition of Ni and/or Cu [38]. On the other hand, XPS results showed the presence of ionic tin, which acts as a Lewis acid, polarizing the C═O bond of furfural, facilitating its hydrogenation. A higher tin concentration does not improve the catalytic performance. Thus, there appears to be a compromise between the dilution of Ru sites, active for the hydrogenation reaction, and the promoter effect of Sn. The RuSn phase inferred from XPS results, is very important towards the activity in the FF hydrogenation. Nevertheless, when the proportion of the Sn(0) increases ($RuSn_{0.8}$ catalyst) the activity decreases, so the formation of the RuSn phase must be kept relatively low with respect to the active metal, so that the catalytic performance would not be affected. In this same sense, Wang et al. have demonstrated by calculations using the density functional theory (DFT) that the reactivity of furfural depends on the coverage of the surface with hydrogen, going through a maximum to intermediate values of coverage [39].

Scheme 1 shows a simplified reaction pathway for the hydrogenation of furfural. Hydrogenation of the C═O bond of FF and of the furan ring gives rise to furfuryl alcohol (FFA) and tetrahydrofurfural (THFF), respectively. Further hydrogenation of any of these two compounds generates tetrahydrofurfuryl alcohol (THFA). In addition, many other reactions can take place, such as the hydrogenolysis of the C═O bond, decarbonylation, furan ring opening, etc. Also, some condensation products of high molecular weight have been reported [40,41].

Table 3 shows the selectivity values for the different reaction products obtained with Ru/C, $RuSn_{0.4}/C$ and $RuSn_{0.8}/C$ catalysts

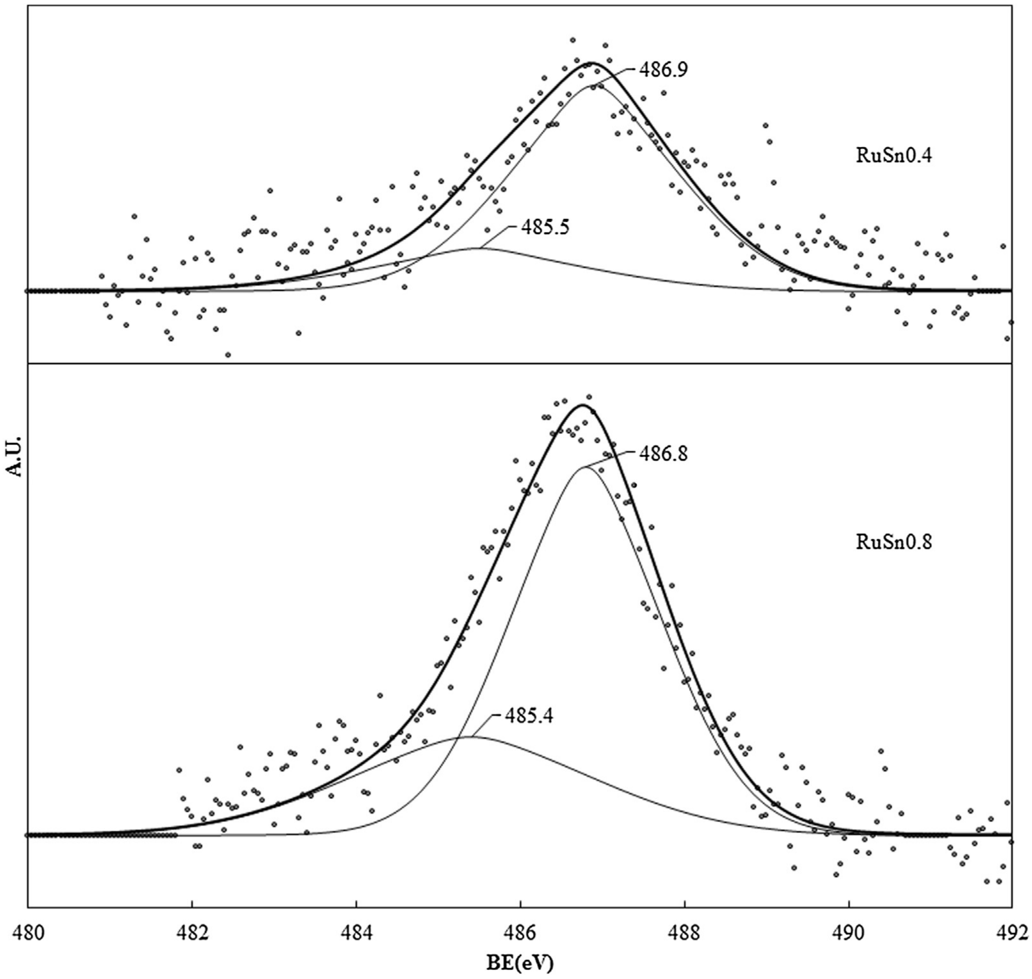

Fig. 4. XPS spectra of Sn $3d_{5/2}$ level for $RuSn_{0.4}/C$ and $RuSn_{0.8}/C$ bimetallic catalysts.

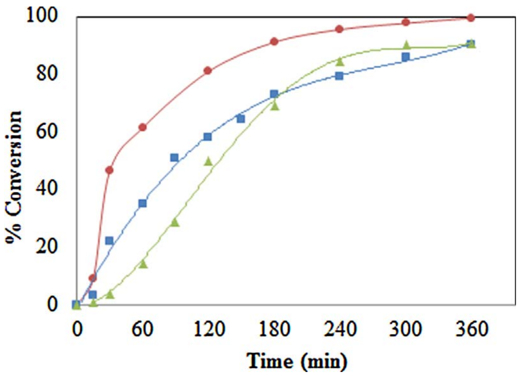

Fig. 5. Aqueous Phase Hydrogenation of furfural: (■) Ru/C, (●) $RuSn_{0.4}/C$ and (▲) $RuSn_{0.8}/C$ (90 °C and 1.25 MPa H_2).

corresponding to the maximum conversion achieved by each of them. Ru/C catalyst presented a low selectivity to FFA (47% at 85% conversion). This result is due to the formation of undesirable products, among which THFA, cyclopentanone (obtained by rearrangement of furan ring by water effect), 1,5-pentanediol, etc., can be mentioned.

Concerning the bimetallic systems, the results of selectivity to FFA are much higher, especially in the case of $RuSn_{0.4}/C$ catalyst. These results suggest that the hydrogenation of furfural proceeds through different adsorbed intermediates, depending on the nature of the catalytic surface. The classical studies of Delbecq and Sautet for the understanding of the selectivity during the hydrogenation of α,β-unsaturated aldehydes suggest that the competitive adsorption of C=C and C=O groups is dependent on the radial expansion of the *d* orbitals of the metal [42]. Thus, the higher the expansion of the *d* orbitals, the greater the electronic repulsion with the C=C bond and therefore the lower the probability of adsorption through a planar geometry, leading to a higher selectivity towards the hydrogenation of the C=O bond. The *d* band width of Ru is smaller than the corresponding to metals such as Pt or Ir, then it is expected that in this case, the adsorption of furfural molecule through the carbonyl group would not be favored, thus obtaining a low selectivity to the unsaturated alcohol.

One very well-known way to improve the selectivity towards hydrogenation of the carbonyl group is to promote the base metal with a second one [43,44]. In this sense, in the case of the present paper the modification of the active sites of ruthenium by the addition of tin would favor the appearance of adsorbed species of the type η1-(O) and η2-(C,O) that lead to the preferential hydrogenation of the carbonyl group, with the consequent increase in the selectivity towards FFA. According to XPS results, the electronic effects exerted by tin on ruthenium are also important. This is possible due to the creation of a new type of active site, as a consequence of the specific interaction between $SnBu_4$ and the supported and reduced Ru. The close proximity of both metals demonstrated by TPR, supports this hypothesis.

Tabla 3 shows the selectivity towards the desired product, furfuryl alcohol, for two different conversion levels. It can be seen that the selectivity towards FFA for the $RuSn_{0.4}/C$ catalyst remains at a high level (over 85%), throughout the experiment. Just as it was observed with the activity of the catalysts, a higher addition of tin reduces the selectivity to FFA, which may be due to the lowered number of active sites.

Table 3
Catalytic performance of Ru/C, $RuSn_{0.4}/C$ and $RuSn_{0.8}/C$ catalysts in the APH of furfural (FF) [T = 90 °C, pH_2 = 1.25 MPa, $W_{cat.}$ = 250 mg, V_{FF} = 0.45 mL, V_{water} = 50 mL].

Catalyst	r_i[a]	TOF[b]	X^c_{FF} (%)	S^d_{FFA} (%)	S^e_i (%)				
					THF	THFF	THFA	FFA	Others
Ru/C	3.5	0.52	85	99	2	0	15	47	36
RuSn0.4	10.8	2.21	95	91	0	1	1	90	8
RuSn0.8	3.0	0.43	90	95	0	2	25	62	11

[a] Initial reaction rate of FF (mmol gRu^{-1} min^{-1}).
[b] Turnover frequency ($min-^{1}$).
[c] Conversion of furfural after 5 h of reaction.
[d] Selectivity to furfuryl alcohol at 10% conversion of furfural.
[e] Selectivity to product *i* at maximum conversion (THF = tetrahydrofuran; THFF = tetrahydrofurfural; THFA = tetrahydrofurfuryl alcohol; FFA = furfuryl alcohol).

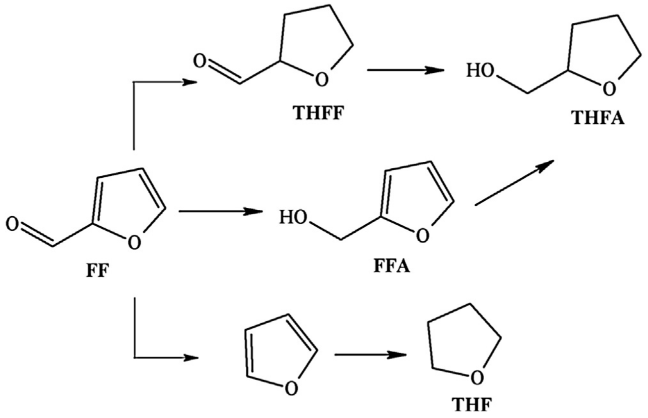

Scheme 1. A schematic pathway for the hydrogenation of furfural.

Finally, to investigate their reusability, a sample of each of the tested catalysts was used repeatedly in the aqueous-phase hydrogenation of furfural at 90 °C and a H_2 pressure of 1.25 MPa. As shown in Fig. 6a–c, a significant drop in furfural conversion was observed after the catalyst was reused twice. This drop in conversion could be due to the polymerization of furfural under the reaction conditions. These oligomers could not have been removed from the surface by a simple washing with water. One remarkable aspect is that the selectivity to FFA kept high values during all the reuses. Anyway, additional spectroscopic and thermogravimetric studies are needed to explain this behavior.

4. Conclusions

The aqueous-phase hydrogenation (APH) of furfural has been investigated using a Ru catalyst promoted with Sn added through SOMC/M techniques. The levels of Sn/Ru atomic ratios selected varied between 0.1 and 0.8. The monometallic Ru/C catalysts showed a high level of activity, but the selectivity to furfuryl alcohol reached a value of only 47%. The electronic properties of ruthenium seem to be responsible for this behavior. The addition of tin has different effects on the Ru/C system, both in terms of conversion and selectivity, depending on its concentration. There seems to be a compromise between the dilution of Ru sites, active for the hydrogenation reaction, and the promoter effect of Sn. The high furfuryl alcohol selectivity achieved with the $RuSn_{0.4}/C$ catalyst demonstrated the promising potential of this system in APH reactions, especially considering that it also displayed a high reactivity at the same time. The close interaction between tin and ruthenium, leading to a well-defined active phase as measured by XPS, would be responsible for this behavior.

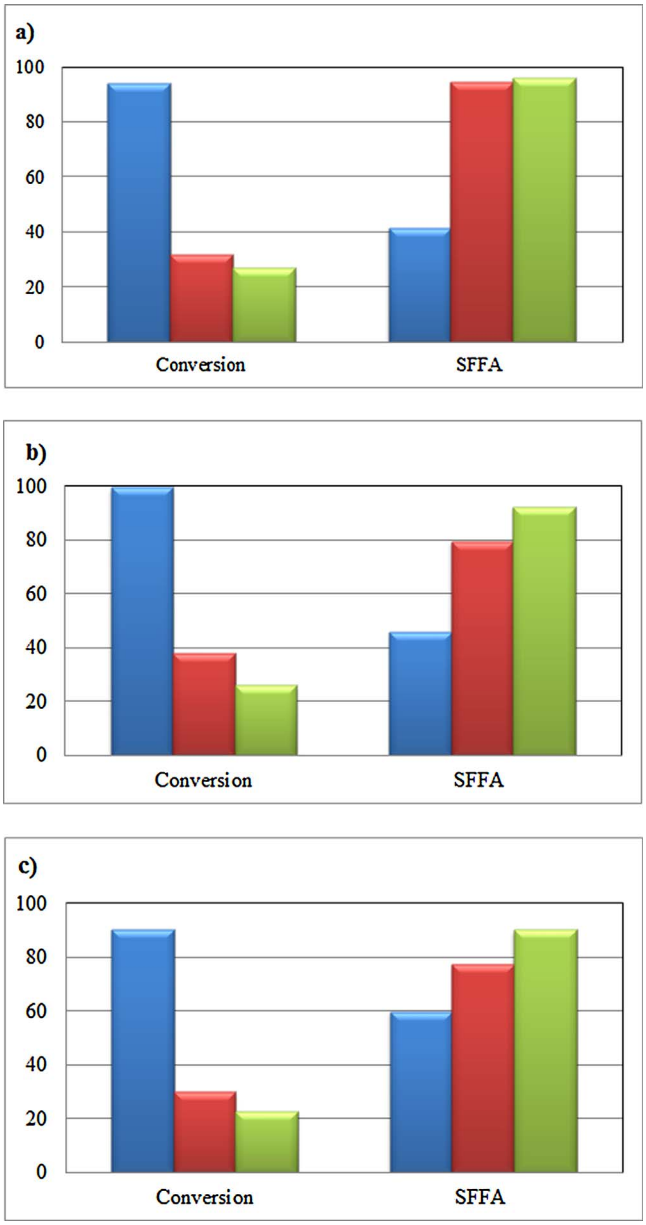

Fig. 6. Conversion and selectivity to furfuryl alcohol (FFA) in the APH of furfural (FF) at 90 °C and 1.25 MPa H_2 for (a) Ru/C, (b) $RuSn_{0.4}/C$ and (c) $RuSn_{0.8}/C$ ((■) fresh catalyst; (■) 1st. reuse and (■) 2nd. reuse).

Acknowledgements

The authors would like to thank the following institutions of Argentina for funding this work: Consejo Nacional de Investigaciones Científicas y Técnicas (CONICET) (PIP 0276), Universidad Nacional de La Plata (Project X 700), Universidad Nacional del Noroeste de la

Provincia de Buenos (Project SIB 2924/14) and Secretaría de Políticas Universitarias del Ministerio de Educación (Project Resolution N° 115/2015). Thanks are given to ANPCyT for the purchase of the SPECS multitechnique analysis instrument (PME8-2003).

References

[1] S. Sorrell, J. Speirs, R. Bentley, A. Brandt, R. Miller, Energy Policy 38 (2010) 5290–5295.
[2] M.I. Jahirul, M.G. Rasul, A.A. Chowdhury, N. Ashwath, Energies 5 (2012) 4952–5001.
[3] R.A. Sheldon, J. Mol. Catal. A: Chem. 422 (2016) 3–12.
[4] B. Kamm, M. Kamm, Appl. Microbiol. Biotechnol. 64 (2004) 137–145.
[5] A.S. Mamman, Bioprod. Biofuels Biorefin. 2 (2008) 438–454.
[6] D.M. Alonso, J.Q. Bond, J.A. Dumesic, Green Chem. 12 (2010) 1493–1513.
[7] C.M. Cai, T. Zhang, R. Kumar, C.E. Wyman, J. Chem. Technol. Biotechnol. 89 (2014) 2–10.
[8] B. Kamm, P.R. Gruber, M. Kamm, Biorefineries-Industrial Processes and Products: Status Quo and Future Directions, Wiley-VCH, 2005.
[9] A. Corma, S. Iborra, A. Velty, Chem. Rev. 107 (2007) 2411–2502.
[10] B. Nagaraja, V. Kumar, V. Shasikala, A. Padmasri, B. Sreedhar, Catal. Commun. 4 (2003) 287–293.
[11] Á. O'Driscoll, J.J. Leahy, T. Curtin, Catal. Today 279 (2017) 194–201.
[12] M.M. Villaverde, T.F. Garetto, A.J. Marchi, Catal. Commun. 58 (2015) 6–10.
[13] A.B. Merlo, V. Vetere, J.F. Ruggera, M.L. Casella, Catal. Commun. 10 (2009) 1665–1669.
[14] J. Lee, Y. Xu, G.W. Huber, Appl. Catal. B: Environ. 140–141 (2013) 98–107.
[15] C. Especel, D. Duprez, F. Eeprom, C.R. Chimie, 17 (2014) 790–800.
[16] J. Fontana, C. Vignado, E. Jordao, F.C.A. Figueiredo, W.A. Carvalho, Catal. Today 172 (2011) 27–33.
[17] B.A. Riguetto, C.E.C. Rodrigues, M.A. Morales, E. Baggio-Saitovitch, L. Gengembre, E. Payen, C.M.P. Marques, J.M.C. Bueno, Appl. Catal. A: Gen. 318 (2007) 70–78.
[18] Y. Pouilloux, F. Autin, C. Guimon, J. Barrault, J. Catal. 176 (1998) 215–224.
[19] A.M. Silva, O.A.A. Santos, M.A. Morales, E.M. Baggio-Saitovitch, E. Jordao, M.A. Fraga, J. Mol. Catal. A: Chem. 253 (2006) 62–69.
[20] B.F. Machado, M. Oubenali, M.R. Axet, T.T.N. Guyen, M. Tunckol, M. Girleanu, O. Ersen, I.C. Gerber, P. Serp, J. Catal. 309 (2014) 185–198.
[21] O.A. Ferretti, M.L. Casella, Controlled preparation of heterogeneous catalysts, in: M. Basset, R. Psaro, D. Roberto, R. Ugo (Eds.), Modern Surface Organometallic Chemistry, Wiley-VCH Verlag GmbH, Weinheim, 2009, pp. 239–291.
[22] D. Baudouin, J.-P. Candy, U. Rodemerck, F. Krumeich, L. Veyre, P.B. Webb, C. Thieuleux, C. Copéret, Catal. Today 235 (2014) 237–244.
[23] H.P. Bideberripe, J.M. Ramallo-López, S.J.A. Figueroa, M.A. Jaworski, M.L. Casella, G.J. Siri, Catal. Commun. 12 (2011) 1280–1285.
[24] H.R. Adúriz, C.E. Gígola, A.M. Sica, M.A. Volpe, R. Touroude, Catal. Today 15 (1992) 459–467.
[25] F. Humblot, D. Didillon, F. Lepeltier, J.P. Candy, J. Corker, O. Clause, F. Bayard, J.M. Basset, J. Am, Chem. Soc. 120 (1998) 137–146.
[26] G.F. Santori, M.L. Casella, G.J. Siri, H.R. Adúriz, O.A. Ferretti, Appl. Catal. A: Gen. 197 (2000) 141–149.
[27] A.B. Merlo, B.F. Machado, V. Vetere, J.L. Faria, M.L. Casella, Appl. Catal. A: Gen. 383 (2010) 43–49.
[28] E. Bailón-García, F. Carrasco-Marín, A.F. Pérez-Cadenas, F.J. Maldonado-Hodar, Appl. Catal. A: Gen. 512 (2016) 63–73.
[29] B. Bachiller-Baeza, A. Guerrero-Ruiz, P. Wang, I. Rodríguez-Ramos, J. Catal. 204 (2001) 450–459.
[30] S.G. Wettstein, J.Q. Bond, D.M. Alonso, H.N. Pham, A.K. Datye, J.A. Dumesic, Appl. Catal. B: Environ. 117–118 (2012) 321–329.
[31] G.J. Siri, J.M. Ramallo-López, M.L. Casella, J.L.G. Fierro, F.G. Requejo, O.A. Ferretti, Appl. Catal. A: Gen. 278 (2005) 239–249.
[32] J.A. Rodriguez, T. Jirsak, S. Chaturvedi, J. Hrbek, J. Am. Chem. Soc. 120 (1998) 11149–11157.
[33] C.D. Wagner, SRD-20 X-ray Photoelectron Spectroscopy Database. (version 1.0), National Institute of Standards and Technology (NIST), Gaithersburg, MD, 1989.
[34] J. Lee, Y.T. Kim, G.W. Huber, Green Chem. 16 (2014) 708–718.
[35] R.M. Mironenko, O.B. Belskaya, T.I. Gulyaeva, A.I. Nizovskii, A.V. Kalinkin, V.I. Bukhtiyarov, A.V. Lavrenov, V.A. Likholobov, Catal. Today 249 (2015) 145–152.
[36] S. Xia, Y. Li, Q. Shang, C. Zhang, P. Ma, Trans. Tianjin Univ. 22 (2016) 202–210.
[37] L. Chen, B. Zhang, X. Zhang, X. Guo, Scientific Reports, (2016), http://dx.doi.org/10.1038/srep28558 www.nature.com/scientificreports.
[38] C. Zhang, Q. Lai, J.H. Holles, Catal. Commun. 89 (2017) 77–80.
[39] S.G. Wang, V. Vorotnikov, D.G. Vlachos, ACS Catal. 5 (2015) 104–112.
[40] J. Kijenski, P. Winiarek, T. Paryjczak, A. Lewicki, A. Mikołajska, Appl. Catal. A: Gen. 233 (2002) 171–182.
[41] H.Y. Zheng, Y.L. Zhua, B.T. Teng, Z.Q. Bai, C.H. Zhang, H.W. Xiang, Y.W. Li, J. Mol. Catal. A: Chem. 246 (2006) 18–23.
[42] F. Delbecq, P. Sautet, J. Catal. 152 (1995) 217–236.
[43] F. Delbecq, P. Sautet, J. Catal. 220 (2003) 115–126.
[44] G. Neri, L. Mercadante, C. Milone, R. Pietropaolo, S. Galvagno, J. Mol. Catal. A: Chem. 108 (1996) 41–50.